1. PanMagnesium

Thermodynamic database for multi-component magnesium-rich casting and wrought alloys

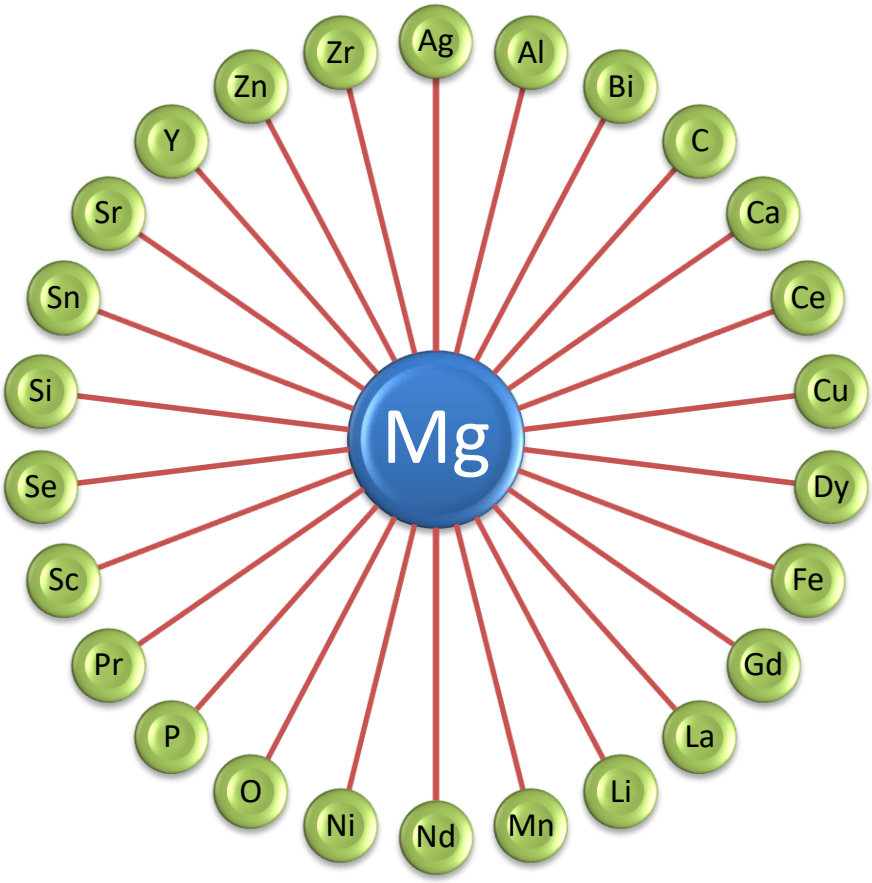

Copyright © CompuTherm LLC

1.1 Components

Total of **27** components are included in the database as listed here:

Ag-Al-Bi-C-Ca-Ce-Cu-Dy-Fe-Gd-La-Li-**Mg**-Mn-Nd-Ni-O-P-Pr-Sc-Se-Si-Sn-Sr-Y-Zn-Zr

1.2 Suggested Composition Range

The suggested composition range for each element is listed in Table 1.1. It should be noted that this given composition range is rather conservative. It is derived from the chemistries of the multicomponent commercial alloys that have been used to validate the current database. In the subsystems, many of these elements can be applied to a much wider composition range. In fact, some subsystems are valid in the entire composition range as given in section 1.5.

Table 1.1: Suggested composition range

Element	Type	Composition Range (wt%)
Mg	Base	70~100
Ag, Al, Ca, Ce, Cu, Fe, Gd, La, Li, Mn, Nd, Ni, Sc, Si, Sn, Sr, Y, Zn, Zr	Major (19)	0~15
Bi, Dy, Pr	Minor (3)	0~2
C, O, P, Se	Trace (4)	0~0.5

There is no composition limit for most binary and many ternary systems formed with major components. These subsystems are valid in the full composition range from 0-100% as detailed in Table 1.4 ~ Table 1.7 below. More restrictions apply to minor and trace components in Table 1.1. Oxygen containing systems are generally restricted to solid oxides and temperature below 1000°C, only the Mg-Ca-O and Si-O systems include the liquid oxide.

1.3 What's new in PanMg2020

PanMg2020 constitutes a major upgrade compared to the previous version PanMg2019. An effort was made to upgrade Ag, Fe, Ni, Sc, and Zr from the class of minor to major alloying components by full assessment of 21 new binary systems and improvement of 7 binary systems. A conservative expansion of suggested composition range from 10 to 15 wt.% for major components was made. Now the comprehensive matrix of binaries with all major alloying components is clearly covering this complete 20-component subset. The binary systems comprising minor and trace components are considered separately.

Key improvements include:

- 21 new binary system descriptions of Al-C , Ag-Fe, Ag-La, Ag-Ni, Ag-Sc, Ag-Sr, Ca-Sc, Ce-Fe, Fe-Sc, Fe-Y, La-Mn, La-Sc, La-Sn, Li-Sc, Sc-Si, Sc-Sn, Sc-Sr, Sc-Zn, Sc-Zr, Sn-Y, Sr-Y.
- One new ternary system description of Al-C-Mg.
- Improvement and correction of seven binary systems Al-C, Al-Ni, Cu-Sn, Fe-Ni, Mg-Si, Mg-Zr, Sc-Y.

1.4 Phases

Total of **574 phases** are included in the database. The phase names are selected according to the following strict rules in Table 1.2 for consistent and intuitive phase identification in different categories. In the category of solid solution phases, indicated in the TDB Viewer of Pandat as CEF(SLN), we distinguish

SE = Solution phase extending to at least one stable phase of an elemental component, disordered.

SI = Solution intermetallic phase usually described by a model with more than one sublattice.

In the category of **stoichiometric** phases (fixed composition) the **TDB Viewer** of Pandat displays **CEF(ST*)**, where * indicates the number of components:

ST1 = Unary stoichiometric phase

ST2 = Binary stoichiometric phase

ST3 = Ternary stoichiometric phase

ST4 = Quaternary stoichiometric phase.

Table 1.2: Rules for phase names in PanMg

Category	**Rule for phase name**
SE solution CEF(SLN)	Structure names of all solution phases stable as **Element**: Bcc, Bct, Cbcc, Dhcp, Fcc, Gas, Hcp, Liquid, Rhomb, Si_diam. Phase Cub (A13) is stable as βMn.
SI solution CEF(SLN)	Name = **Selected** approximate chemical stoichiometric formula. • Name is selected close to an important/dominant binary or ternary intermetallic phase with approximate stoichiometry: Al12Mg17, R5Mg41, ... • Name always starts with first element. Elements alphabetical (AlFe, not FeAl). Exceptions: **rare earth** – metal – **non-metal**. • Wild card "elements" R, M, X are used for extended solution ranges: **R** = Rare earth element (La, Ce,..., Lu)*, **M** = metal, **X** = non-metal (C, N, O, F, P, S, Cl, As, Se, Br, Sb, Te, I)**. Examples: RAl, RCu6, RMg, RMg12, Mg2M • Phases may be distinguished/marked by affix for **crystal structure**: MgZn2_C14, MgZn2_C36, ..., AlCaMg_C36, R8Mg70Zn6_14H • Phase name may be **crystal prototype name**, such as CaCu5;

	that phase is stable as binary CaCu5, CeCu5, Cu5Gd, LaCu5, Cu5Nd, CaNi5,CeNi5, LaNi5, GdNi5, and NdNi5. • Temperature **polymorphs** may be distinguished by affix _T1, _T2, _T3, ...: R3Al11_T1 (low temperature), R3Al11_T2 (high temperature). • **Well established phase names** might be given as affix, upper case: RM3_W, YZn5_H, ... or with first three letters of the established Greek symbol, lower case: AlMgZn_phi, AlMgZn_tau, AlCu_eps, AlCu_gam1, AlCu_gam2
Stoichiometric CEF(ST1), CEF(ST2), CEF(ST3), CEF(ST4)	Name = **Chemical stoichiometric formula**. • Name always starts with first element. Elements generally alphabetical; Exceptions: rare earth element (La, Ce, Pr, Nd, Sm, Eu, Gd, Tb, Dy, ... Lu) FIRST; non-metal (C, N, O, F, P, S, Cl, As, Se, Br, Sb, Te, I) LAST. Examples: AgCa, **Ce**Ag, MgSc, Si**C**, Si3**N**4, Al4Si**C**4, Y2**O**3 • Temperature **polymorphs** of same stoichiometry are distinguished by affix ..._T* Zn3Zr_T1 (low temperature), Zn3Zr_T2 (high temperature) • **Well established phase names** might be given as affix, upper case: Mg58Y8Zn6_18R, Mg46Y8Zn6_10H Stable **elements** (ST1) are C_graph, Se_A8, and P_ red (P_ white is metastable).

**) Rare earth elements do not include Sc and Y; Lanthanides only R = (La, Ce, Pr, Nd, Sm, Eu, Gd, Tb, Dy, Ho, Er,Tm, Yb, Lu).*

***) Non-metals are from "Pettifor-string", chemical order from 88 to 102, (Sb, As, P, Te, Se, S, C, I, Br, Cl, N, O, F), and listed according to the periodic table.*

The total **574** phases assessed in PanMg2020 comprise the **182** solution phases (gas phase, liquid, plus 180 solid solution phases) and **392** stoichiometric phases. These 392 comprise 4 unary, 310 binary, 76 ternary, and 2 quaternary assessed stoichiometric phases.

As an illustration of the names and models assigned to the various solution and stoichiometric phases a small representative selection is listed in Table 1.3. For all **574** phases assessed in PanMg2020 this information can be displayed in the TDB viewer of Pandat or be found at www.computherm.com.

Table 1.3: Example of phase names and related information

Name	Model	Lattice Size	Constituent
Gas	GAS	(1)	(Ag,Al,Al2,Bi,Bi2,C,C2,C3,C4,C5,Ca,Ce,Cu,Cu2,Dy,Fe,Gd,La,Li,Li2,Mg,Mg2,Mn,Nd,Ni,P,P2,P4,Pr,Sc,Sc2,Se,Se2,Se3,Se4,Se5,Se6,Se7,Se8,Si,Si2,Si3,Si4,Sn,Sr,Y,Zn,Zr,AlC,CSi,CSi2,C2Si,Li3C,Li4C,Li6C,O,O2,O3,Al2O,Al2O2,Al2O3,AlO,AlO2,C2O,C3O2,CO,CO2,CaO,CeO,CuO,FeO,La2O,La2O2,LaO,Li2O,Li2O2,LiO,MgO,NdO,NdO2,NiO,PrO,ScO,SeO,SeO2,SiO,SiO2,Sn2O2,Sn3O3,Sn4O4,SnO,SnO2,Sr2O,SrO,YO,ZrO,ZrO2)
Liquid	CEF (SLN)	(1)(0.5)	(Ag,Al,Bi,Bi2Mg3,C,Ca,Ca2Sn,CaO,Ce,Cu,Dy,Fe,Gd,La,LaSn,Li,Li2C2,Li4Sn,Mg,Mg2Sn,MgO,Mn,O,P,Nd,Ni,Pr,Sc,Se,Si,Sn,Sr,Y,Zn,Zr)
Hcp	CEF (SLN)	(1)(0.5)	(Ag,Al,Bi,Ca,Ce,Cu,Dy,Fe,Gd,La,Li,Mg,Mn,Nd,Ni,O,Pr,Sc,Se,Si,Sn,Sr,Y,Zn,Zr)(Va)
Al12Mg17	CEF (SLN)	(10)(24)(24)	(Mg)(Al,Ca,Cu,Li,Mg,Zn)(Al,Cu,Mg,Zn)
Al11Mn4_T1	CEF (SLN)	(11)(4)	(Al)(Fe,Mn)
Al11Mn4_T2	CEF (SLN)	(29)(10)	(Al,Mn)(Mn)
Al2Ca_C15	CEF (SLN)	(0.666667)(0.333333)	(Al,Mg)(Ca,Sr)

CaCu5	CEF (SLN)	(0.166667)(0.833333)	(Ca,Ce,La,Gd,Nd,Y)(Al,Cu,Ni)
CaMgO_halite	CEF (SLN)	(1)(1)	(Ca,Mg)(O)
GdMg2_C15	CEF (SLN)	(0.333333) (0.666667)	(Gd,Y)(Li,Mg,Zn)
RZn2	CEF (SLN)	(0.333333) (0.666667)	(Ce,Gd,La,Nd)(Zn)
R5Mg41	CEF (SLN)	(5)(41)	(Ca,Ce,La,Nd,Y)(Mg,Zn)
Si_diam	CEF (SLN)	(1)	(Al,C,Li,O,P,Si,Sn,Zn)
Se_A8	CEF (ST1)	(1)	(Se)
Ag2Ca	CEF (ST2)	(0.666667) (0.333333)	(Ag)(Ca)
Al2CaSi2	CEF (ST3)	(0.4)(0.2)(0.4)	(Al)(Ca)(Si)
Al17Cu9Mg45Si29	CEF (ST4)	(0.17)(0.09) (0.45)(0.29)	(Al)(Cu)(Mg)(Si)

**For liquidus projection calculations it is usually recommended to suspend the gas phase*

1.5 Key Elements and Subsystems

The modeling status for the constituent binaries, ternaries and quaternaries is given in Table 1.4 ~ Table 1.7. All binary systems for the **20**-component **subset**, including Mg and major components, are listed in Table 1.4. Modeled binary systems including at least one of the minor or trace components defined in Table 1.1 are given in Table 1.5. Thermodynamic descriptions for ternary systems are indicated in Table 1.6. Thermodynamic descriptions validated or extended for quaternary systems are indicated in Table 1.7.

The color represents the following meaning:

: Full description

: Full description for major phases

: Extrapolation

Table 1.4: Modeling quality status of binary systems in the **20**-component **subset** formed from combinations of Mg with all major components.

	Al	**Ca**	**Ce**	**Cu**	**Fe**	**Gd**	**La**	**Li**	**Mg**	**Mn**	**Nd**	**Ni**	**Sc**	**Si**	**Sn**	**Sr**	**Y**	**Zn**	**Zr**
Ag	Ag-Al	Ag-Ca	Ag-Ce	Ag-Cu	Ag-Fe	Ag-Gd	Ag-La	Ag-Li	Ag-Mg	Ag-Mn	Ag-Nd	Ag-Ni	Ag-Sc	Ag-Si	Ag-Sn	Ag-Sr	Ag-Y	Ag-Zn	Ag-Zr
Al		Al-Ca	Al-Ce	Al-Cu	Al-Fe	Al-Gd	Al-La	Al-Li	Al-Mg	Al-Mn	Al-Nd	Al-Ni	Al-Sc	Al-Si	Al-Sn	Al-Sr	Al-Y	Al-Zn	Al-Zr
Ca			Ca-Ce	Ca-Cu	Ca-Fe	Ca-Gd	Ca-La	Ca-Li	Ca-Mg	Ca-Mn	Ca-Nd	Ca-Ni	Ca-Sc	Ca-Si	Ca-Sn	Ca-Sr	Ca-Y	Ca-Zn	Ca-Zr
Ce				Ce-Cu	Ce-Fe	Ce-Gd	Ce-La	Ce-Li	Ce-Mg	Ce-Mn	Ce-Nd	Ce-Ni	Ce-Sc	Ce-Si	Ce-Sn	Ce-Sr	Ce-Y	Ce-Zn	Ce-Zr
Cu					Cu-Fe	Cu-Gd	Cu-La	Cu-Li	Cu-Mg	Cu-Mn	Cu-Nd	Cu-Ni	Cu-Sc	Cu-Si	Cu-Sn	Cu-Sr	Cu-Y	Cu-Zn	Cu-Zr
Fe						Fe-Gd	Fe-La	Fe-Li	Fe-Mg	Fe-Mn	Fe-Nd	Fe-Ni	Fe-Sc	Fe-Si	Fe-Sn	Fe-Sr	Fe-Y	Fe-Zn	Fe-Zr
Gd							Gd-La	Gd-Li	Gd-Mg	Gd-Mn	Gd-Nd	Gd-Ni	Gd-Sc	Gd-Si	Gd-Sn	Gd-Sr	Gd-Y	Gd-Zn	Gd-Zr
La								La-Li	La-Mg	La-Mn	La-Nd	La-Ni	La-Sc	La-Si	La-Sn	La-Sr	La-Y	La-Zn	La-Zr
Li									Li-Mg	Li-Mn	Li-Nd	Li-Ni	Li-Sc	Li-Si	Li-Sn	Li-Sr	Li-Y	Li-Zn	Li-Zr
Mg										Mg-Mn	Mg-Nd	Mg-Ni	Mg-Sc	Mg-Si	Mg-Sn	Mg-Sr	Mg-Y	Mg-Zn	Mg-Zr
Mn											Mn-Nd	Mn-Ni	Mn-Sc	Mn-Si	Mn-Sn	Mn-Sr	Mn-Y	Mn-Zn	Mn-Zr
Nd												Nd-Ni	Nd-Sc	Nd-Si	Nd-Sn	Nd-Sr	Nd-Y	Nd-Zn	Nd-Zr
Ni													Ni-Sc	Ni-Si	Ni-Sn	Ni-Sr	Ni-Y	Ni-Zn	Ni-Zr
Sc														Sc-Si	Sc-Sn	Sc-Sr	Sc-Y	Sc-Zn	Sc-Zr
Si															Si-Sn	Si-Sr	Si-Y	Si-Zn	Si-Zr
Sn																Sn-Sr	Sn-Y	Sn-Zn	Sn-Zr
Sr																	Sr-Y	Sr-Zn	Sr-Zr
Y																		Y-Zn	Y-Zr
Zn																			Zn-Zr

Table 1.5: Modeled binary systems formed with remaining minor and trace components Bi, C, Dy, O, P, Pr, and Se.

Al-Bi	Bi-Sn	C-Li	**Mg**-O	P-Si
Al-C	Bi-Zn	C-**Mg**	**Mg**-P	
Al-P	Ca-O	C-Si	**Mg**-Pr	
Bi-**Mg**	Ca-P	C-Sn	**Mg**-Se	
Bi-O	C-Ca	Dy-**Mg**	O-Si	

Total of **189 binary systems** are modeled (marked green or yellow). In the 20-component subset of Table 1.5, 168 of the possible 190 binary systems or **88%** are modeled.

The same color code is used to indicate the quality of modeled ternary and quaternary systems in Table 1.6 ~ Table 1.7. Total of **108 ternary systems** and **17 quaternary systems** are modeled.

Table 1.6: Modeled Ternary Systems

Ag-Al-Cu	Al-Cu-Mn	Al-**Mg**-Zn	Ce-**Mg**-Mn	La-**Mg**-Zn
Ag-Al-**Mg**	Al-Cu-Nd	Al-Mn-Sc	Ce-**Mg**-Nd	Li-**Mg**-Mn
Ag-Cu-**Mg**	Al-Cu-Si	Al-Mn-Si	Ce-**Mg**-Sn	Li-Si-Sn
Ag-**Mg**-Nd	Al-Cu-Sn	Al-Nd-Y	Ce-**Mg**-Y	Li-**Mg**-Si
Al-Bi-**Mg**	Al-Cu-Zn	Al-Si-Y	Ce-**Mg**-Zn	Li-**Mg**-Zn
Al-C-**Mg**	Al-Fe-Mn	Al-Si-Zn	Cu-Fe-Si	**Mg**-Mn-Sc
Al-C-Si	Al-Fe-Si	Al-Sn-Zn	Cu-La-Ni	**Mg**-Mn-Si
Al-Ca-Ce	Al-Gd-La	Bi-**Mg**-Sn	Cu-Li-**Mg**	**Mg**-Mn-Sr
Al-Ca-Fe	Al-Gd-**Mg**	C-Li-Si	Cu-**Mg**-Ni	**Mg**-Mn-Y
Al-Ca-Li	Al-Gd-Nd	C-Li-Sn	Cu-**Mg**-Si	**Mg**-Mn-Zn
Al-Ca-**Mg**	Al-Gd-Y	Ca-Ce-**Mg**	Cu-**Mg**-Y	**Mg**-Mn-Zr
Al-Ca-Si	Al-La-Nd	Ca-Fe-Si	Cu-**Mg**-Zn	**Mg**-Nd-Y
Al-Ca-Sr	Al-La-Y	Ca-Li-**Mg**	Cu-Ni-Si	**Mg**-Nd-Zn
Al-Ce-Gd	Al-Li-**Mg**	Ca-Li-Si	Cu-Sn-Zn	**Mg**-Ni-Si
Al-Ce-La	Al-Li-Mn	Ca-**Mg**-O	Fe-**Mg**-Si	**Mg**-Si-Sn
Al-Ce-**Mg**	Al-Li-Si	Ca-**Mg**-Si	Fe-Mn-Si	**Mg**-Si-Zn
Al-Ce-Nd	Al-**Mg**-Mn	Ca-**Mg**-Sn	Gd-Li-**Mg**	**Mg**-Sn-Zn
Al-Ce-Si	Al-**Mg**-Sc	Ca-**Mg**-Sr	Gd-**Mg**-Mn	**Mg**-Y-Zn
Al-Ce-Y	Al-**Mg**-Si	Ca-**Mg**-Zn	Gd-**Mg**-Y	**Mg**-Y-Zr
Al-Cu-Gd	Al-**Mg**-Sn	Ca-Sr-Zn	Gd-**Mg**-Zn	Mn-Y-Zr
Al-Cu-Li	Al-**Mg**-Sr	Ce-La-**Mg**	La-**Mg**-Nd	
Al-Cu-**Mg**	Al-**Mg**-Y	Ce-Li-Mn	La-**Mg**-Si	

Table 1.7: Modeled Quaternary Systems

Ag-Al-Cu-**Mg**
Al-Ca-Ce-**Mg**
Al-Ca-Li-**Mg**
Al-Ce-Li-**Mg**
Al-Bi-**Mg**-Sn
Al-Cu-**Mg**-Si
Al-Cu-**Mg**-Zn
Al-Fe-Mn-Si
Al-Li-**Mg**-Si
Al-**Mg**-Mn-Zn
Ca-Ce-**Mg**-Sn
Ca-**Mg**-Si-Sn
Ce-Gd-**Mg**-Y
Ce-**Mg**-Mn-Sc
Gd-**Mg**-Mn-Sc
Mg-Mn-Sc-Y
Mg-Mn-Y-Zr

1.6 Database Validation

The early development of the Mg-database, starting in 1995, is described in [2001Sch] and aspects of quality assurance were first given by [2005Sch].

Progress in systematic development and applications of the current thermodynamic database for Mg alloys is reported in detail in [2018Sch] and [2019Sch]. Models for multicomponent alloys are built in a methodical approach from quantitative descriptions of unary, binary and ternary subsystems [2012Sch]. For a large number of ternary—and some higher—alloy systems, an evaluation of the modeling depth is made with concise reference to experimental work validating these thermodynamic descriptions. A special focus is on ternary intermetallic phase compositions. These comprise solutions of the third component in a binary compound as well as truly ternary solid solution phases, in addition to the simple ternary stoichiometric phases. Concise information on the stability ranges is given. That evaluation is extended to selected quaternary and even higher alloy systems. Thermodynamic descriptions of intermetallic solution phases guided by their crystal structure are also elaborated and the diversity of such unified phases is emphasized [2012Sch].

Key issues in this large thermodynamic Mg alloy database are consistency, coherency and quality assurance. These issues and the basic concept are elaborated in [2013Gro]. The structurally supported modeling, especially of pertinent solid phases, requires proper consideration of multicomponent solid solutions of intermetallic phases which are abundant in magnesium alloys. Moreover, evidence on the database application by predicting phase formation during solidification or heat treatment in advanced multicomponent magnesium alloys from thermodynamic calculations is given in detail in [2013Gro]. Highlights of the most recent progress are given in [2015Sch1].

The growing modeling depth of the PanMagnesium database enhances predictive type calculations of phase formation during solidification, heat treatment or other processing steps of Mg alloys. Evidence is given by

comparing the results of such calculations with the phase formation reported in studies of advanced magnesium alloys, such as Mg—Zn--Y/Zr/Gd/Ce/Nd, Mg—Al—Ca/Mn/Sr/Sn, Mg—Sn—Ca and higher order Mg—Al—Sn—Ca/Sr and Mg—Sn—Ca--Ce/Gd/Zr alloys [2013Gro]. Reference is made to the extensive material provided in that most current publication which is not repeated here.

The current thermodynamic database for magnesium alloys has also been extensively tested and validated using published experimental data [1998Lia, 1999Gro, 2001Gro4, 2001Gro6, 2001Kev1, 2001Kev2, 2001Kev3, 2002Gro1, 2002Gro2, 2003Gro1, 2003Gro2, 2004Bru, 2004Kev, 2004Gro, 2006Ohn4]. Some sub-quaternary systems of this database have been critically assessed: Mg-Al-Ca-Ce, Mg-Al-Ca-Li, Mg-Al-Ce-Li, Mg-Al-Cu-Zn, Mg-Mn-Y-Zr. The quaternary systems Mg-Al-Li-Si [2001Kev4] and Mg-Ce-Mn-Sc, Mg-Gd-Mn-Sc, Mg-Mn-Sc-Y [2000Pis2, 2001Gro2] were thermodynamically modeled and used for technical applications.

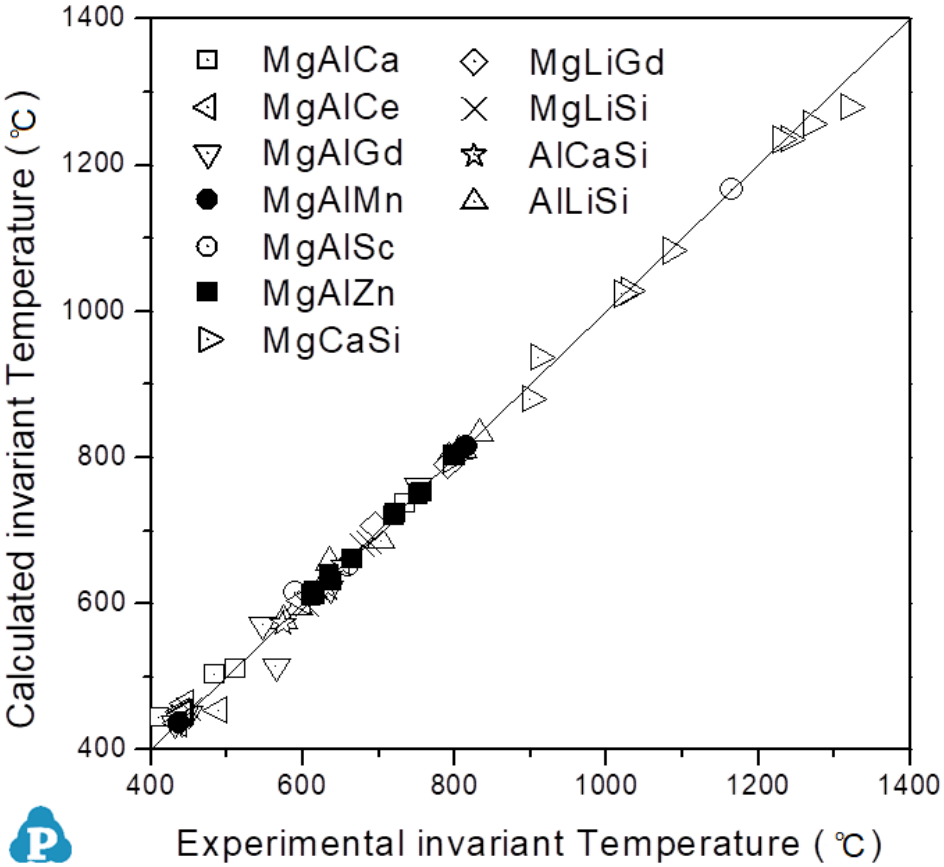

Figure 1.1: Invariant temperatures for various ternary alloys included in PanMagnesium: Comparison between calculated and experimental data.

For the reliability of the calculated phase diagrams the fitting of the invariant temperatures are of paramount importance. Since the measured temperatures of the invariant reactions are not affected by super-cooling related problems, these nonvariant data are perfect criteria for comparison of experimental with calculated data (as shown in Figure 1.1).

For the Mg-Al-Mn system the reliability is checked in detail [2005Ohn]. The liquidus surface of the Mg-rich corner is shown in Figure 1.2. The same experimental data are plotted in Figure 1.3 as comparison between calculated results and experimental data.

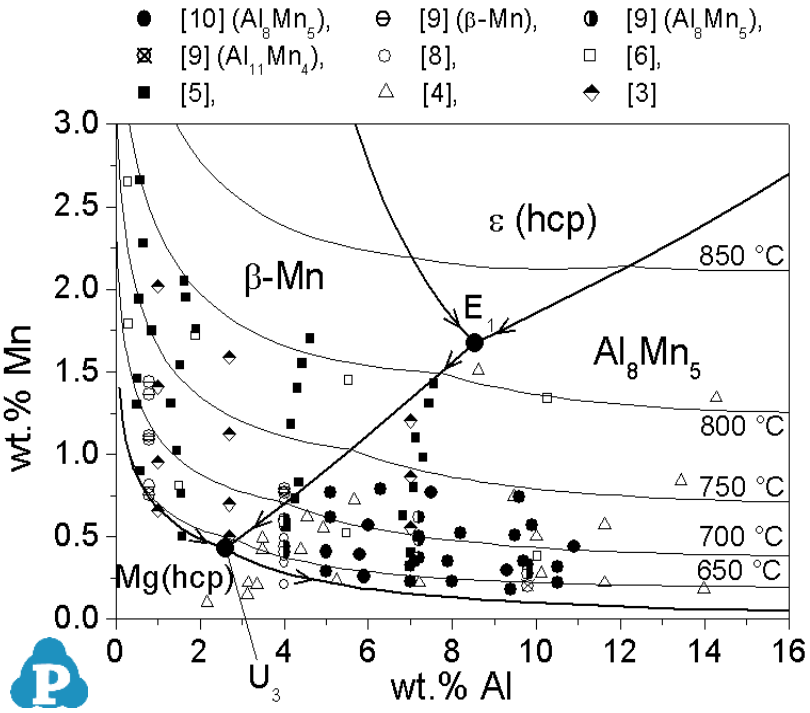

Figure 1.2: Calculated partial liquidus surface, the thick lines indicate monovariant reaction lines and the thin lines represents the isotherms. Superimposed are the compositions of experimental alloys further compared to calculated data of the liquidus surface. The primary solid phase is specified in some experimental data.

This comparison in Figure 1.3 enables easy identification of those groups of experimental data that are not consistent with the bulk of experimental work. There is a reasonable agreement with this bulk of experimental data

and the calculated values. Moreover, there is a reasonable agreement with the primary solidifying phases as shown in Figure 1.2.

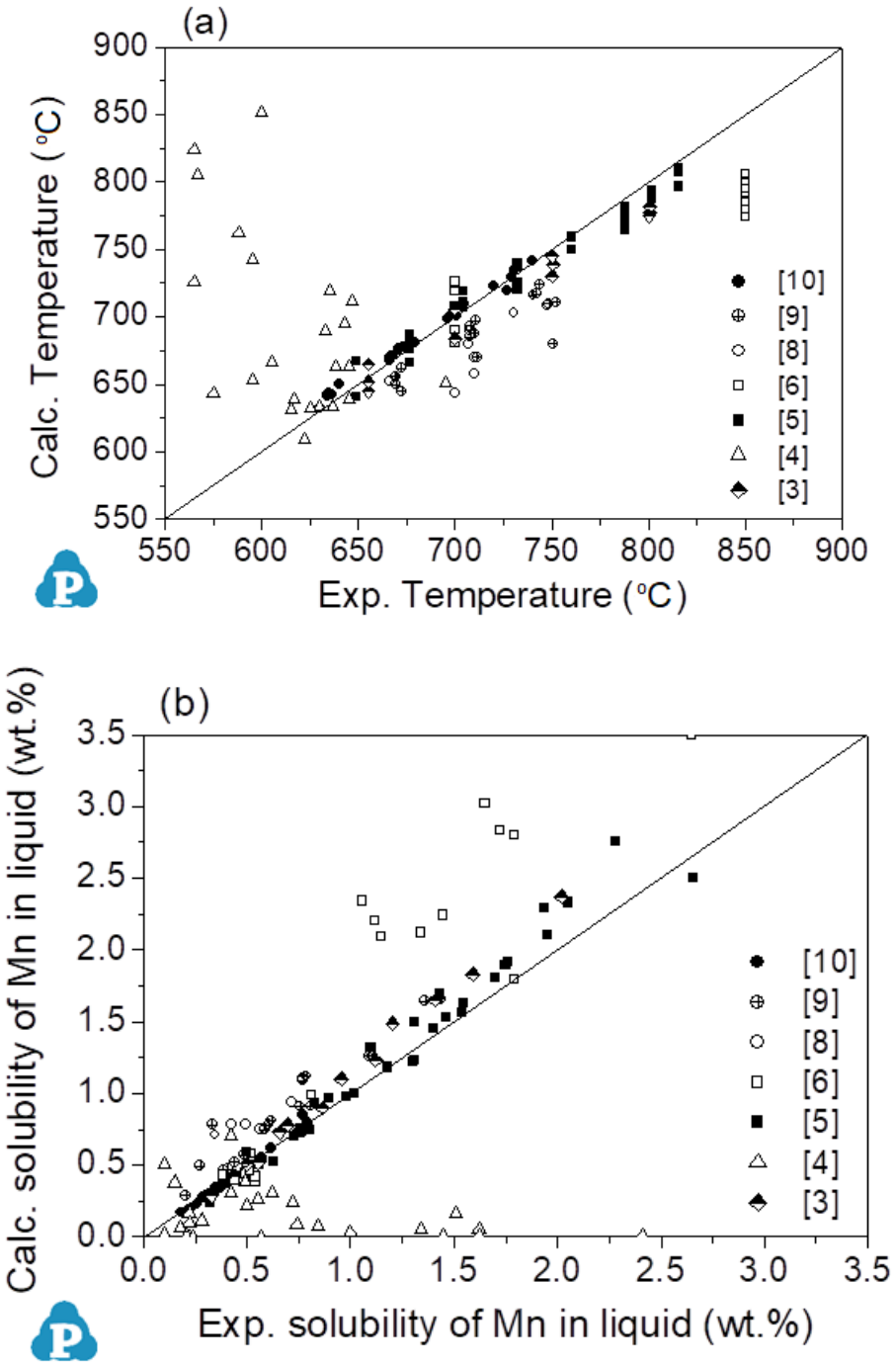

Figure 1.3: Comparison between calculated results and experimental data for all alloy samples in the Mg-Al-Mn system. (a) Liquidus temperature at a given composition, (b) Solubility of Mn in liquid at a given temperature and Al composition. The straight line in Figs. (a) and (b) is a visual aid corresponding to perfect agreement between experimental values and the calculated results from the present thermodynamic model.

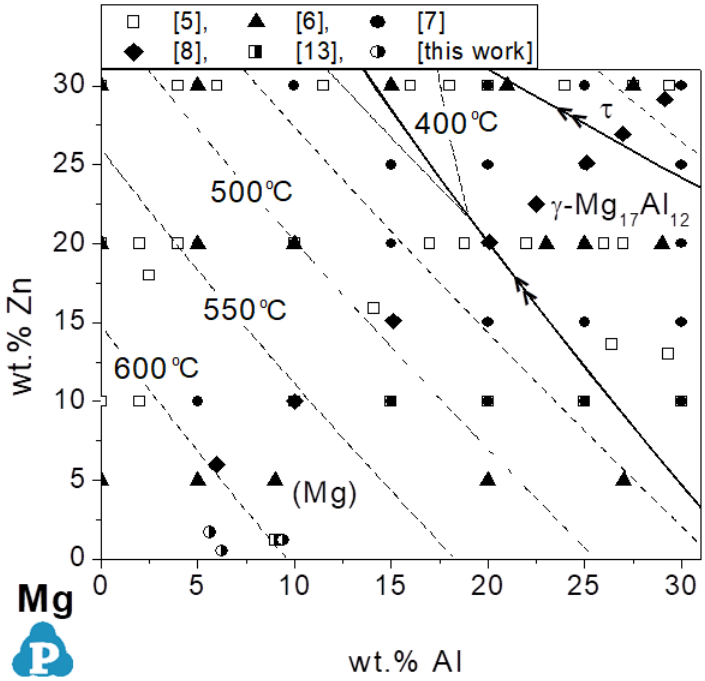

Figure 1.4: Calculated partial Mg–Al–Zn liquidus surface and experimental alloy compositions. The thick lines indicate monovariant reaction lines and the dashed lines represent isotherms at an interval of 50°C.

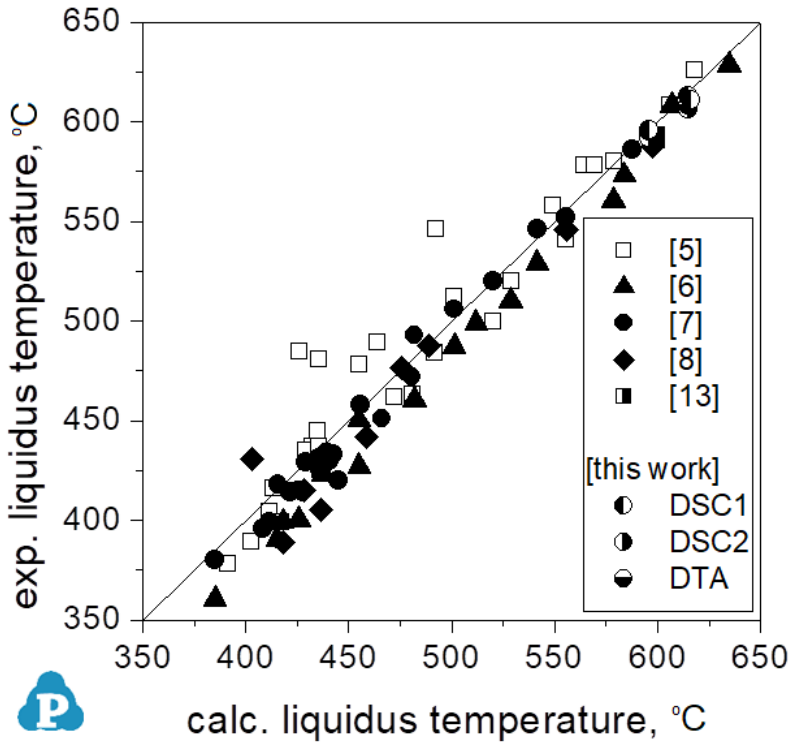

Figure 1.5: Comparison between calculated and experimental liquidus temperature for all alloy samples in the Mg-Al-Zn system. The straight line is a visual aid corresponding to perfect agreement between experimental and calculated results.

The experimental data for the commercially very important Mg-Al-Zn alloys are shown in Figure 1.4 [2006Ohn1]. The liquidus surface of the Mg-rich corner is given in Figure 1.4. The same experimental data is plotted in Figure 1.5 as comparison between calculated results and experimental data. A similar comparison was done for the Mg-rich phase equilibria of the Mg-Mn-Zn system [2006Ohn2]. Technical important liquidus and Solidus temperatures of Mg-rich Mg-Al-Mn-Zn Alloys (AZ series) were investigated by [2006Ohn3].

Measured liquidus temperatures for other ternary Mg-alloy systems are compared in Figure 1.6 with calculations from the magnesium database. These miscellaneous Mg-X1-X2 systems include the alloying elements Al, Ca, Ce, Gd, Li, Sc, and Si.

Additionally a selected comparison of experimental data and calculated phase equilibria is given below. This demonstrates the feasibility to perform reasonable calculations with PanMagnesium even in some very high alloyed regions with vanishing Mg-content as outlined in Table 1.6. For the Al-Li-Si system a comparison between calculated and experimentally measured DTA data is given in Figure 1.7 [2001Gro6]. Figure 1.8 shows a calculated vertical section in the Al-Ce-Si system at constant 90at%Al including the DSC/DTA signals measured [2004Gro].

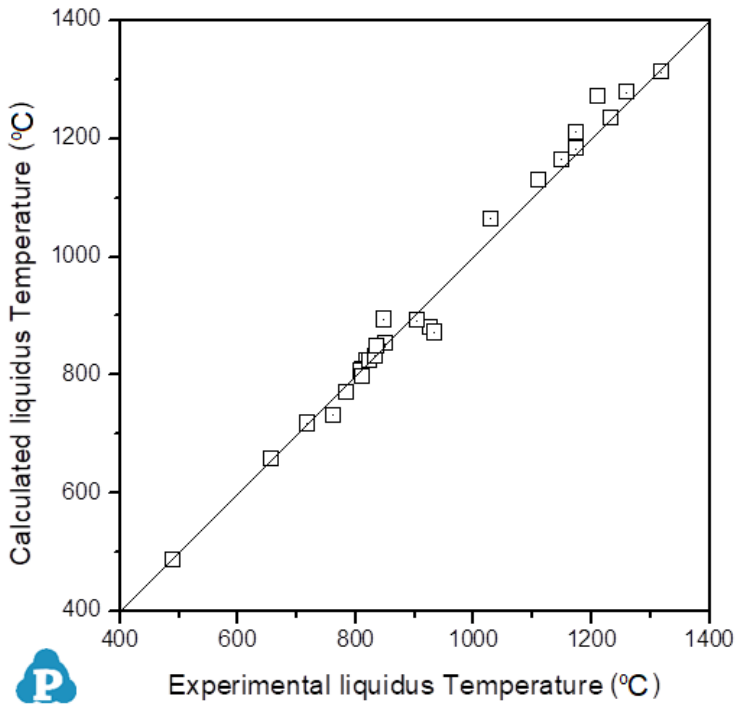

Figure 1.6: Liquidus temperatures for various ternary magnesium alloys outside the Mg-Al-Mn-Zn system, with alloying elements Al, Ca, Ce, Gd, Li, Sc, Si: Comparison between calculated and experimental data.

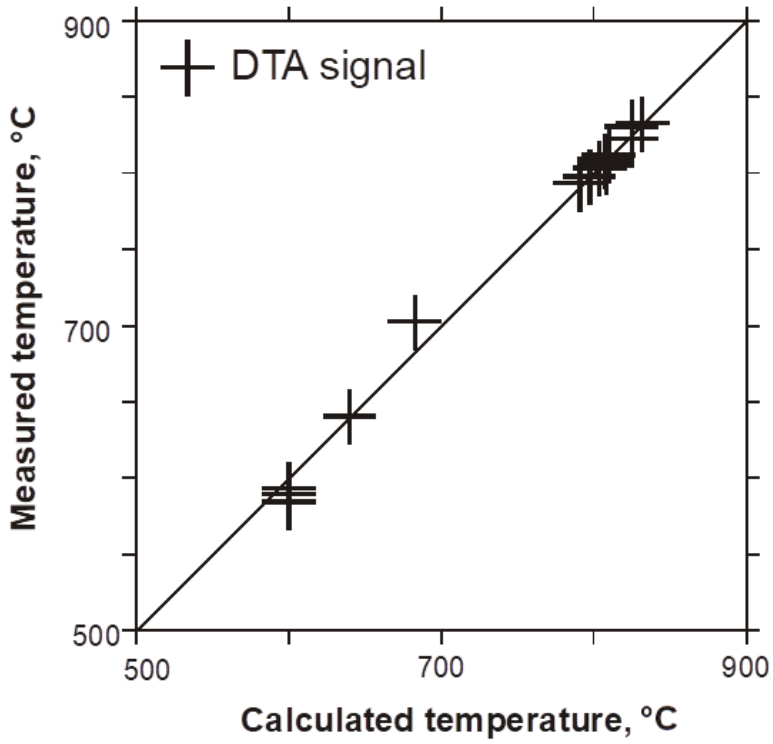

Figure 1.7: Comparison between calculated and experimentally measured DTA data for the Al-Li-Si system [2001Gro6].

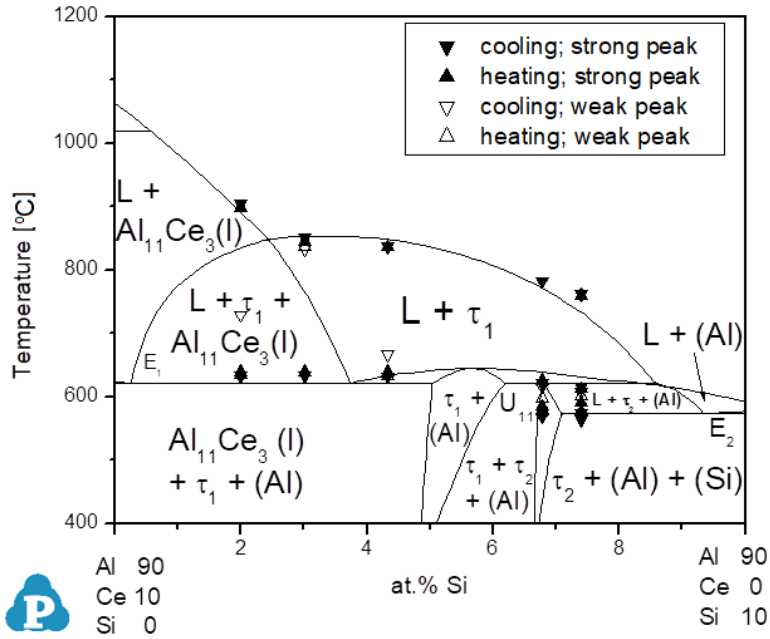

Figure 1.8: Calculated vertical section Al90Ce10 - Al90Si10 at constant 90at%Al including the DSC/DTA signals measured in [2004Gro].

Advanced Mg alloys employing Long Period Stacking Order (LPSO) and icosahedral precipitate phases for superior properties have been studied in detail recently in the most important ternary alloy systems Mg-Gd-Zn [2015Gro] and Mg-Y-Zn [2015Sch2].

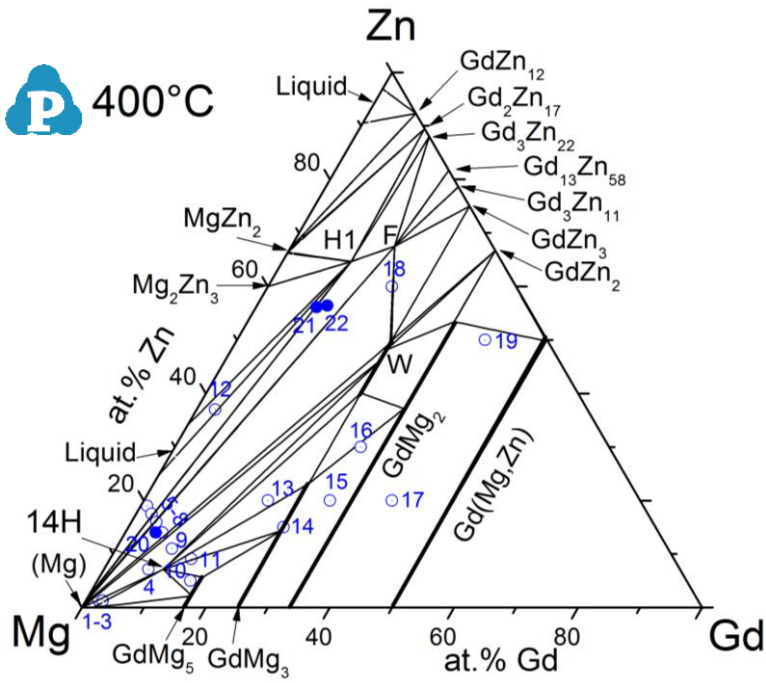

Figure 1.9: Calculated Mg-Gd-Zn isothermal section at 400°C including the sample compositions investigated in [2015Gro].

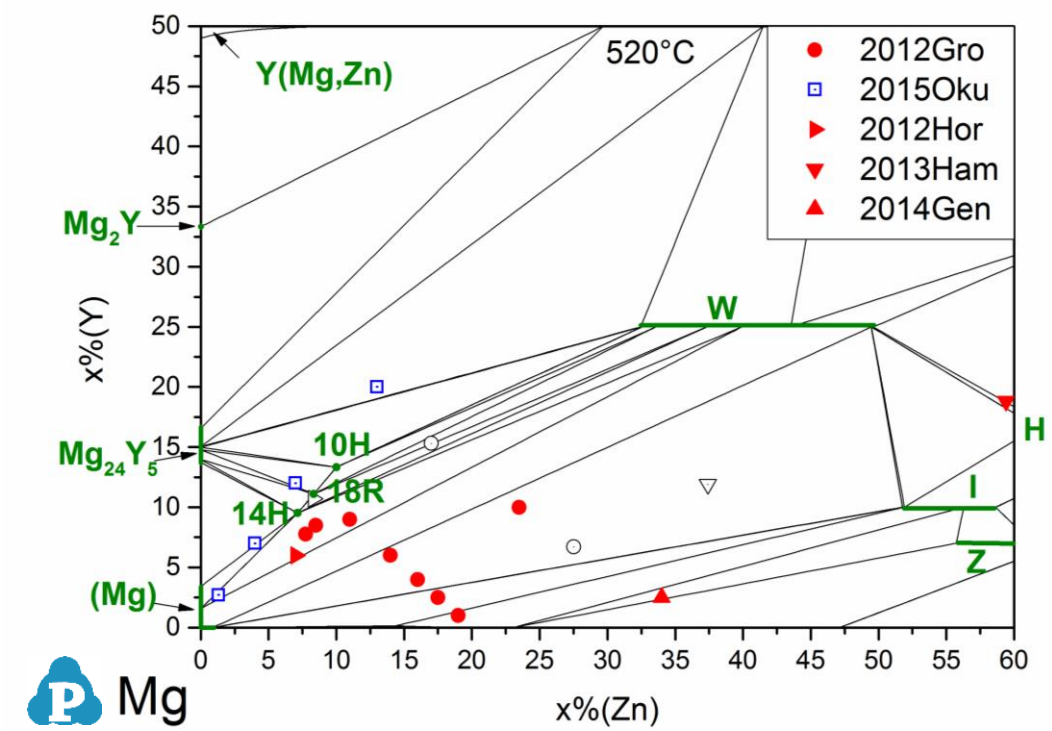

Figure 1.10: Calculated partial Mg-rich Mg-Zn-Y isothermal section at 520°C including sample compositions analyzed in [2015Sch2].

These validated thermodynamic descriptions are embedded in PanMg2020, enabling simulations of related multicomponent alloys. As an example two calculated isothermal sections are shown in Figure 1.9 and Figure 1.10 in comparison with experimental data.

Another highlight of PanMg2020 is the incorporation of oxygen as an element and all relevant solid oxides and gas species. For example, the reaction of Mg with CaO during melting and solidification was studied experimentally and the thermodynamic description of the Mg-Ca-O system was developed with scrutinized oxide data. The calculated isothermal section in Figure 1.11 is also validated using *in-situ* synchrotron radiation diffraction [2018Lia1, 2018Lia2].

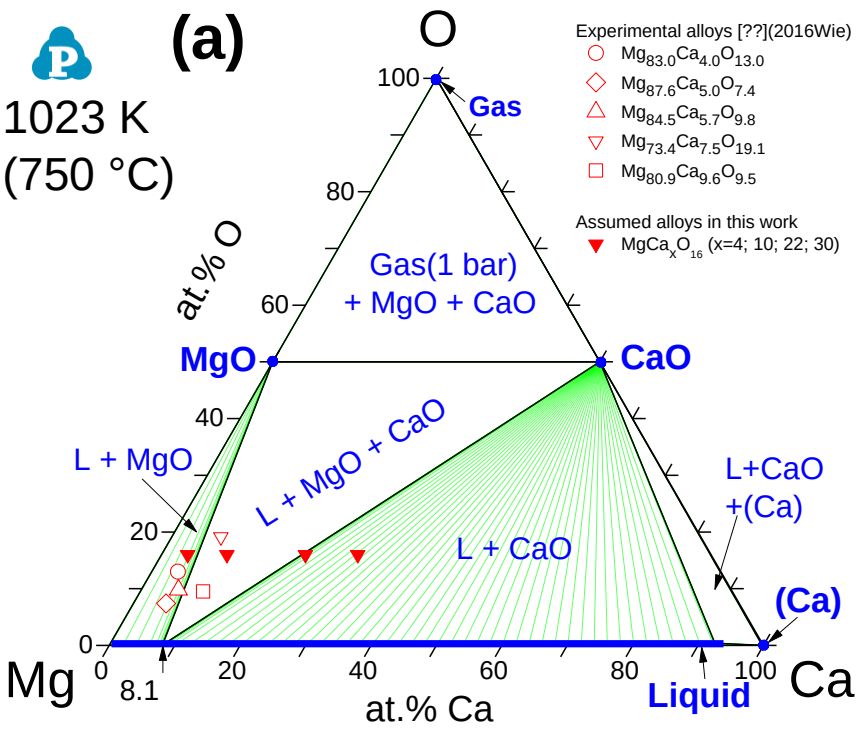

Figure 1.11: Calculated isothermal section of the Mg-Ca-O system, validated using in-situ synchrotron radiation diffraction [2017Lia].

The good agreement between experimental and calculated results, as shown in all of the above figures indicates the reliability of the current PanMagnesium thermodynamic database. Additional validation is given in some comprehensive studies [2012Sch, 2013Gro]. Applications are highlighted in [2018Sch].

1.7 References

[1998Lia] Liang, P., Tarfa, T., Robinson, J.A., Wagner, S., Ochin, P., Harmelin, M.G., Seifert, H.J., Lukas, H.L., Aldinger, F., Experimental investigation and thermodynamic calculation of the Al-Mg-Zn system, Thermochim. Acta 314, 87-110 (1998).

[1999Gro] Gröbner, J., Schmid-Fetzer, R., Pisch, A., Cacciamani, G., Riani, P., Ferro, R.: Experimental Investigations and Thermodynamic Calculation in the Al-Mg-Sc System. Z. Metallkd. 90(11), (1999), S. 872-880.

[2000Pis2] Pisch, A., Gröbner, J., Schmid-Fetzer, R.: Application of Computational Thermochemistry to Al- and Mg-alloy processing with Sc additions. Mat. Sci. Eng. A 289, (2000), S. 123-129.

[2001Gro2] Gröbner, J., Pisch, A., Schmid-Fetzer, R.: Selection of Promising Quaternary Candidates from Mg-Mn-(Sc, Gd, Y, Zr) for Development of Creep-resistant Magnesium Alloys. J. Alloys Comp. 320/2, (2001) 296-301.

[2001Gro4] Gröbner, J., Kevorkov, D., Schmid-Fetzer, R.: Thermodynamic Calculation of Al-Gd and Al-Gd-Mg Phase Equilibria Checked by Key Experiments. Z. Metallkd. 92 (2001) S. 22-27.

[2001Gro6] Gröbner, J., Kevorkov, D., Schmid-Fetzer, R.: The Al-Li-Si System, Part 2: Experimental study and Thermodynamic Calculation of the polythermal equilibria. J. Solid State Chem. 156 (2001) S. 506-511.

[2001Kev1] Kevorkov, D., Gröbner, J., Schmid-Fetzer, R.: The Al-Li-Si system, Part 1: A new structure type Li8Al3Si5 and the ternary solid state phase equilibria. J. Solid State Chem. 156 (2001) S. 500-505.

[2001Kev2] Kevorkov, D.G., Pavlyuk, V.V., Dmytriv, G.S., Bodak, O.I., Gröbner, J., Schmid-Fetzer, R.: The ternary Gd-Li-Mg system: Phase diagram study and computational evaluation. J. Phase Equilibria 22 (1) (2001) S. 34-42.

[2001Kev3] Kevorkov, D., Schmid-Fetzer, R.: The Al-Ca System Part 1: Experimental Investigation of Phase Equilibria and Crystal Structures. Z. Metallkd. 92 (2001) S. 946-952.

[2001Kev4] Kevorkov, D.: Thermodynamics and Phase Equilibria of the Mg-Al-Li-Si System, Ph. D. Thesis TU Clausthal 2001.

[2001Sch] Schmid-Fetzer, R., Gröbner, J.: Focused Development of Magnesium Alloys Using the Calphad Approach. Advanced Engineering Materials 3 (12) (2001) 947-961.

[2002Gro1] Gröbner, J., Schmid-Fetzer, R., Pisch, A., Colinet, C., Pavlyuk, V.V., Dmytriv, G.S., Kevorkov, D.G., Bodak, O.I: Phase equilibria, calorimetric study and thermodynamic modelling of Mg-Li-Ca alloys, Thermochimica Acta 389 (2002) 85-94.

[2002Gro2] Gröbner, J., Schmid-Fetzer, R.:Thermodynamic Modeling of Al-Ce-Mg Phase Equilibria Coupled with Key Experiments, Intermetallics 10 (2002) 415-422.

[2003Gro1] Gröbner, J., Kevorkov, D., Chumak, I. and Schmid-Fetzer, R.: Experimental Investigation and Thermodynamic Calculation of Ternary Al-Ca-Mg Phase Equilibria, Z. Metallkd. 94 (2003) 976-982.

[2003Gro2] Gröbner, J., Kevorkov, D.and Schmid-Fetzer, R.: A new Thermodynamic data set for the binary System Ca-Si and Experimental Investigation in the ternary System Ca-Mg-Si, Intermetallics 11 (2003) 1065-1074.

[2004Bru] Brubaker, C.O., Liu, Z.-K., A computational thermodynamic model of the Ca–Mg–Zn system, J. Alloys Comp. 370, 114-122 (2004).

[2004Gro] J. Gröbner, D. Mirkovic, Rainer Schmid-Fetzer: Thermodynamic Aspects of Constitution, Grain Refining and Solidification Enthalpies of Al-Ce-Si Alloys. Metall. Mater. Trans. A 35A, 3349-3362 (2004).

[2004Kev] Kevorkov, D., Schmid-Fetzer, R. and Zhang F.: Phase Equilibria and Thermodynamics of the Mg-Si-Li System and Remodeling of the Mg-Si System, J. Phase Equil. Diff. 25 (2004) 140-151.

[2005Ohn] M. Ohno, R. Schmid-Fetzer: Thermodynamic assessment of Mg-Al-Mn phase equilibria, focusing Mg-rich alloys. Z. Metallkde. 96, 857-869 (2005).

[2005Sch] R. Schmid-Fetzer, A. Janz, J. Gröbner and M. Ohno: Aspects of quality assurance in a thermodynamic Mg alloy database. Advanced Engineering Materials 7 , 1142-1149 (2005).

[2006Ohn1] M. Ohno, D. Mirkovic and R. Schmid-Fetzer: Phase equilibria and solidification of Mg-rich Mg-Al-Zn alloys. Materials Science & Engineering A, 421, 328-337 (2006).

[2006Ohn2] M. Ohno and R. Schmid-Fetzer: Mg-rich phase equilibria of Mg-Mn-Zn alloys analyzed by computational thermochemistry. Int. J. Materials Research (Z. Metallkunde) 97, 526-532 (2006).

[2006Ohn3] M. Ohno, D. Mirkovic and R. Schmid-Fetzer: Liquidus and Solidus Temperatures of Mg-rich Mg-Al-Mn-Zn Alloys. Acta Materialia, 54, 3883–3891 (2006).

[2006Ohn4] M. Ohno, A. Kozlov, R. Arroyave, Z.K. Liu, and R. Schmid-Fetzer: Thermodynamic modeling of the Ca-Sn system based on finite temperature quantities from first-principles and experiment. Acta Materialia, 54, 4939-4951 (2006).

[2012Sch] R. Schmid-Fetzer, J. Gröbner: Thermodynamic database for Mg alloys — progress in multicomponent modeling. Metals, 2, 377-398 (2012). (Special Issue "Magnesium Technology"), Open Access, www.mdpi.com/2075-4701/2/3/377, dx.doi.org/10.3390/met2030377

[2013Gro] J. Gröbner, R. Schmid-Fetzer: Key issues in a thermodynamic Mg alloy database. Metall. Mater. Trans. A, A44, 2918-2934 (2013) dx.doi.org/10.1007/s11661-012-1483-z

[2015Gro] J. Gröbner, A. Kozlov, X.Y. Fang, S.M. Zhu, J.F. Nie, M.A. Gibson, R. Schmid-Fetzer: Phase equilibria and transformations in ternary Mg–Gd–Zn alloys.Acta Materialia, 90, 400–416 (2015)

[2015Sch1] R. Schmid-Fetzer: Progress in thermodynamic database development for ICME of Mg alloys, in Magnesium Technology 2015, Edited by: M.V. Manuel, A. Singh, M. Alderman, and N.R. Neelameggham,TMS (The Minerals, Metals & Materials Society), 283-287 (2015)

[2015Sch2] Rainer Schmid-Fetzer, Joachim Gröbner, Michiaki Yamasaki, Yoshihito Kawamura, Hiroshi Okuda, Seiji Miura, Toshiaki Horiuchi, Jian-Feng Nie: Thermal stability of Mg-Zn-Y LPSO phases and revised thermodynamic description of the Mg-Zn-Y phase diagram. Mg 2015 - The 10th International Conference on Magnesium Alloys and Their Applications. October 11-16, 2015, Jeju, Korea.Symp. LPSO Structure & Its Related Alloys, Invited, October 12, 2015. eProceedings, EO-3-0372, pp 1-23.

[2018Lia1] S.-M. Liang, A. Kozlov, R. Schmid-Fetzer, The Mg–Ca–O system: Thermodynamic analysis of oxide data and melting/solidification of Mg alloys with added CaO, Int. J. Materials Research (Z. Metallkunde), 109 (2018) 185-200.

[2018Lia2] S.-M. Liang, R. Schmid-Fetzer, Complete thermodynamic description of the Mg-Ca-O phase diagram including the Ca-O, Mg-O and CaO-MgO subsystems, Journal of the European Ceramic Society, 38 (2018) 4768-4785.

[2018Sch] R. Schmid-Fetzer, F. Zhang: The light alloy Calphad databases PanAl and PanMg. Calphad, 61, 246-263 (2018). http://dx.doi.org/10.1016/j.calphad.2018.04.006

[2019Sch] R. Schmid-Fetzer, Recent Progress in Development and Applications of Mg Alloy Thermodynamic Database, in: V.V. Joshi, J.B. Jordon, D. Orlov, N.R. Neelameggham (Eds.) Magnesium Technology 2019, TMS Annual Meeting, Springer International Publishing, 2019, 249-255. https://doi.org/10.1007/978-3-030-05789-3_37